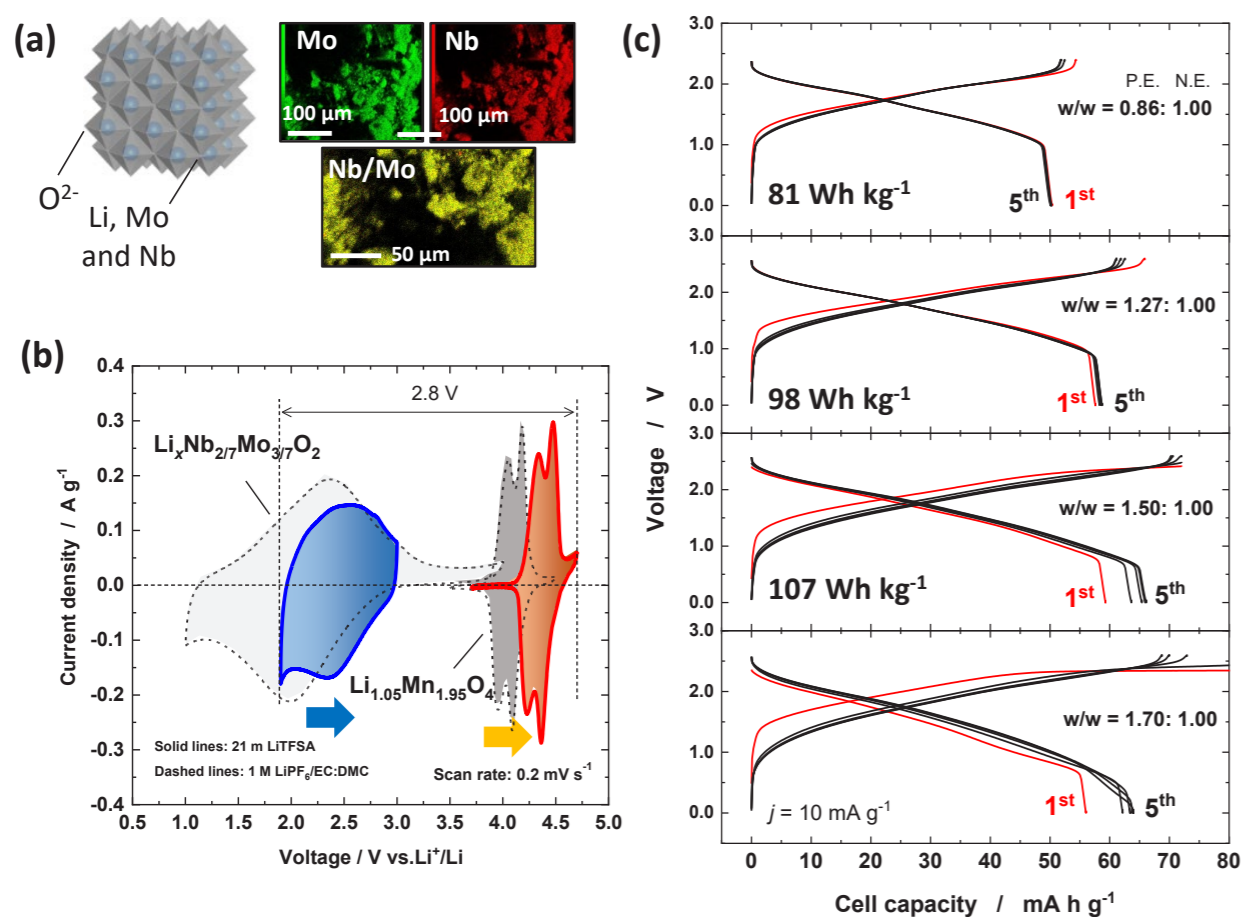


## Nanosized and Metastable Mo Oxides for Aqueous Li-Ion Batteries

The development of safe energy devices is a key challenge, causing strong interest in aqueous Li-ion batteries. Due to the narrow electrochemical stable potential window of aqueous electrolytes, the development of negative electrode materials exhibiting a large capacity and low potential without triggering decomposition of water is crucial. We propose a new negative electrode material,  $\text{Li}_x\text{Nb}_{2/7}\text{Mo}_{3/7}\text{O}_2$ , for high-energy aqueous Li-ion batteries. This oxide delivers a large capacity of  $\sim 170 \text{ mA h g}^{-1}$  with a low operating potential range of 1.9–2.8 versus  $\text{Li}/\text{Li}^+$  in 21 m lithium bis(trifluoromethanesulfonyl) amide (LiTFSA) aqueous electrolyte. X-ray absorption spectroscopy reveals that the large reversible capacity originates from Mo redox reaction in aqueous electrolyte.

There is rising demand for better rechargeable batteries due to the penetration of electric vehicles (EVs) and the installation of stationary energy storage systems (ESSs) for renewable energy provision. Li-ion batteries (LIBs) are the best option thanks to their high energy density and efficiency. However, flammable organic electrolytes in LIBs raise safety concerns upon scaling up, and battery explosion hazards are, therefore, a serious problem. The safety issues can be fundamentally addressed by utilizing non-flammable aqueous electro-

lytes. The first aqueous LIB was reported using  $\text{LiMn}_2\text{O}_4$  and  $\text{VO}_2$  (B) as positive and negative electrodes, respectively [1]. However, the major demerit of aqueous Li-ion batteries is their low operating voltage and thus lower energy density. This problem originates from the thermodynamic limitation (i.e., the narrow electrochemical stability window of aqueous electrolytes, and the operating voltage window is typically  $< 1.8 \text{ V}$ ). In 2015, a new era of high-voltage aqueous LIBs began with the introduction of the so-called “water-in-salt” electrolytes [2].



**Figure 1:** (a) A schematic illustration of the crystal structure energy-dispersive X-ray spectroscopy (EDX) elemental maps of  $\text{Li}_x\text{Nb}_{2/7}\text{Mo}_{3/7}\text{O}_2$ , (b) cyclic voltammograms of  $\text{Li}_{1.05}\text{Mn}_{1.95}\text{O}_4$  and  $\text{Li}_x\text{Nb}_{2/7}\text{Mo}_{3/7}\text{O}_2$  in 21 m LiTFSA (solid lines) and 1 M LiPF<sub>6</sub>/EC:DMC (dashed lines), (c) comparison of charge/discharge curves of  $\text{Li}_{1.05}\text{Mn}_{1.95}\text{O}_4$  and  $\text{Li}_x\text{Nb}_{2/7}\text{Mo}_{3/7}\text{O}_2$  full cells consisting of different weight ratios of positive electrodes to negative electrodes at a rate of  $10 \text{ mA g}^{-1}$ .

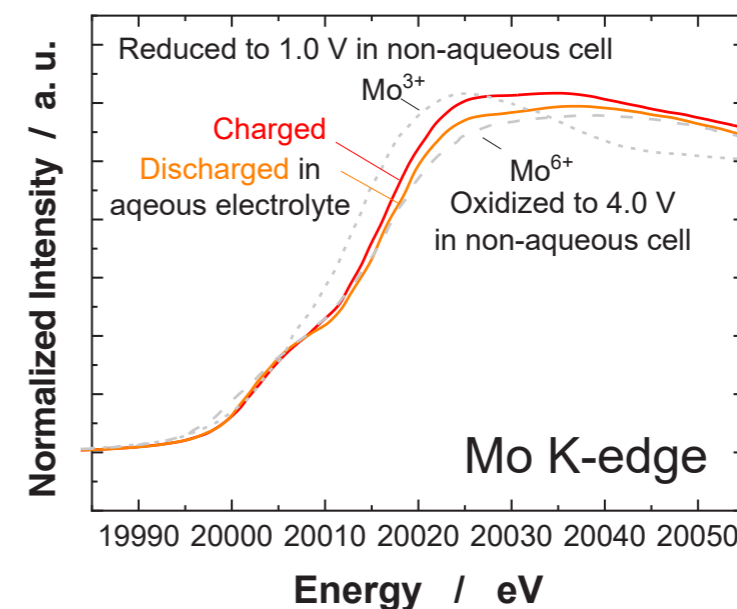


**Figure 2:** Changes in Mo K-edge XAS spectra of  $\text{Li}_x\text{Nb}_{2/7}\text{Mo}_{3/7}\text{O}_2$  after cycling in the aqueous electrolyte. The data collected in nonaqueous electrolyte is also shown for comparison.

A much wider stability window,  $\sim 3 \text{ V}$ , is realized in the water-in-salt electrolyte, i.e., saturated 21 m LiTFSA aqueous electrolyte [2]. A significant reduction of the water concentration effectively suppresses the oxygen evolution reaction, leading to higher decomposition potential upon oxidation. The hydrogen evolution potential on reduction is also shifted toward more negative potentials due to the presence of protective solid electrolyte interphase layers formed by the decomposition of TFSA<sup>-</sup> anions.

In this study, a new negative electrode material exhibiting high capacity and high durability [i.e., a metastable and nanosized molybdenum oxide with a rock-salt structure, Fig. 1(a)] is proposed for aqueous LIBs. Our group originally designed an Li-excess molybdenum oxide containing niobium ions,  $\text{Li}_{9/7}\text{Nb}_{2/7}\text{Mo}_{3/7}\text{O}_2$ , as a high-capacity positive electrode material for nonaqueous batteries [3]. To use  $\text{Li}_{9/7}\text{Nb}_{2/7}\text{Mo}_{3/7}\text{O}_2$  for negative electrode materials, the oxide was treated with water, leading to Mo oxidation and Li extraction coupled with hydrogen generation, forming  $\text{Li}_x\text{Nb}_{2/7}\text{Mo}_{3/7}\text{O}_2$  [4]. Cyclic voltammograms of  $\text{Li}_{1.05}\text{Mn}_{1.95}\text{O}_4$  and  $\text{Li}_x\text{Nb}_{2/7}\text{Mo}_{3/7}\text{O}_2$  in 21 m LiTFSA/water and 1 M LiPF<sub>6</sub>/EC:DMC are compared in Fig. 1(b); the upshift for reaction potentials in the water-in-salt electrolyte originates from the Nernstian shift [2]. Charge/discharge curves of  $\text{Li}_{1.05}\text{Mn}_{1.95}\text{O}_4$  and  $\text{Li}_x\text{Nb}_{2/7}\text{Mo}_{3/7}\text{O}_2$  full cells with different weight ratios of positive electrodes to negative electrodes are shown in Fig. 1(c). When the mass loading ratio of the positive electrode to negative electrode is limited to 0.86, excellent reversibility and a small initial irreversible capacity are noted within a charge/discharge voltage range of

2.4 to 0 V. The average discharge voltage is calculated to be 1.62 V, which is a higher value as aqueous batteries. When the mass ratio is increased to 1.5, the oxide delivers a large capacity of  $\sim 170 \text{ mA h g}^{-1}$ , corresponding to the full cell with high energy density of  $> 100 \text{ W h kg}^{-1}$ .

To further study the charge compensation mechanisms of  $\text{Li}_x\text{Nb}_{2/7}\text{Mo}_{3/7}\text{O}_2$  in aqueous electrolyte, X-ray absorption (XAS) spectra have been collected at beamline BL-9C. As shown in Fig. 2, Mo K-edge XAS spectra show a clear shift in absorption energy upon charge/discharge in the aqueous electrolyte. The change in the oxidation state of Mo is estimated to be one electron redox of Mo ions by comparing the reference materials of fully charged and discharged  $\text{Li}_x\text{Nb}_{2/7}\text{Mo}_{3/7}\text{O}_2$  prepared in nonaqueous electrolyte, which is also consistent with the estimation from the current passed through the electrode material in the cell.

### REFERENCES

- [1] W. Li, J. R. Dahn and D. S. Wainwright, *Science* **264**, 1115 (1994).
- [2] L. Suo, O. Borodin, T. Gao, M. Olguin, J. Ho, X. Fan, C. Luo, C. Wang and K. Xu, *Science* **350**, 938 (2015).
- [3] S. Hoshino, A. M. Glushenkov, S. Ichikawa, T. Ozaki, T. Inamasu and N. Yabuuchi, *ACS Energy Lett.* **2**, 733 (2017).
- [4] J. Yun, R. Sagehashi, Y. Sato, T. Masuda, S. Hoshino, H. B. Rajendra, K. Okuno, A. Hosoe, A. S. Bandarenka and N. Yabuuchi, *PNAS* **118**, e2024969118 (2021).

**BEAMLINE**  
BL-9C

**N. Yabuuchi (Yokohama National Univ.)**